COSMIC RAYS, CLOUDS, AND CLIMATE

NIGEL MARSH and HENRIK SVENSMARK
Danish Space Research Institute,
Juliane Maries Vej 30, DK-2100 Copenhagen Ø, Denmark.

Received: 2 March 2000; Accepted in final form: 10 May 2000

Abstract. A correlation between a global average of low cloud cover and the flux of cosmic rays incident in the atmosphere has been observed during the last solar cycle. The ionising potential of Earth bound cosmic rays are modulated by the state of the heliosphere, while clouds play an important role in the Earth's radiation budget through trapping outgoing radiation and reflecting incoming radiation. If a physical link between these two features can be established, it would provide a mechanism linking solar activity and Earth's climate. Recent satellite observations have further revealed a correlation between cosmic ray flux and low cloud top temperature. The temperature of a cloud depends on the radiation properties determined by its droplet distribution. Low clouds are warm ($>$273 K) and therefore consist of liquid water droplets. At typical atmospheric supersaturations ($\sim$1%) a liquid cloud drop will only form in the presence of an aerosol, which acts as a condensation site. The droplet distribution of a cloud will then depend on the number of aerosols activated as cloud condensation nuclei (CCN) and the level of super saturation. Based on observational evidence it is argued that a mechanism to explain the cosmic ray-cloud link might be found through the role of atmospheric ionisation in aerosol production and/or growth. Observations of local aerosol increases in low cloud due to ship exhaust indicate that a small perturbation in atmospheric aerosol can have a major impact on low cloud radiative properties. Thus, a moderate influence on atmospheric aerosol distributions from cosmic ray ionisation would have a strong influence on the Earth's radiation budget. Historical evidence over the past 1000 years indicates that changes in climate have occurred in accord with variability in cosmic ray intensities. Such changes are in agreement with the sign of cloud radiative forcing associated with cosmic ray variability as estimated from satellite observations.

1. Introduction

The Sun is a variable star, which emits both electromagnetic radiation and energetic particles known as the solar wind – these are released as a plasma carrying a fingerprint of the solar magnetic field throughout inter-planetary space. Effects from the solar wind are felt at distances well beyond Neptune, possibly up to 200 AU from the Sun, in a region of space known as the Heliosphere (Fig. 1). The flux of the inter-planetary magnetic field (IMF) at 1 AU is $\sim$5 nT. Variability in solar activity affects both the radiative output of the Sun and the strength of the IMF carried by the solar wind. The IMF shields the heliosphere from galactic cosmic radiation which consists of energetic particles, mainly protons that are accelerated through stellar processes in our galaxy. Thus, solar variability modulates both the flux of incoming galactic cosmic radiation (GCR) and the amount of solar radiation received by the planets.

Space Science Reviews **94:** 215–230, 2000.

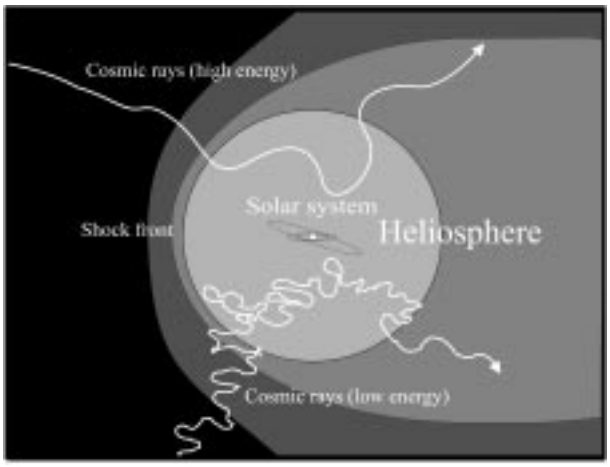

Figure 1. Schematic of Heliosphere

Satellite measurements of total solar radiation over the past 20 years have revealed that the total radiative output of the Sun varies by ∼0.1% (1.4 Wm^{-2}) over a solar cycle (approx. 11 years). Currently this is believed to be too small to significantly influence observed surface temperatures directly, although this may have been larger back in time (Lean et al., 1995). However, the UV region of the solar radiation spectrum is observed to vary by up to 10%. UV is absorbed by ozone and can lead to variations in Stratospheric heating. It has been suggested that variability in this heating due to changes in solar activity can have an influence on the dynamical properties of the troposphere below (Geller and Alpert, 1980; Haigh, 1996; Shindell et al., 1999). It remains to be seen how this affects surface climate once taking into account the many feedback mechanisms involved. GCRs interact with the Earth's atmosphere through nuclear collisions producing secondary particles (protons, neutrons and muons) which can penetrate deeper into the atmosphere; these undergo further collisions, which leads to a cascade of particles. The cascade ends when the nucleonic component i.e., neutrons and protons, have reached energies that are too low for further particle production. The primary energy spectrum results in a maximum production rate at about 16 km. Below 16 km, the charge particle intensity drops off and it is mainly the muons and electrons, products of very high-energy GCR collisions, which contribute to the charged particle intensity at low altitudes (Lal and Peters, 1967; Herman and Goldberg, 1978). Observations of both muons and neutrons at the Earth's surface contain information related to atmospheric ionisation at different altitudes and can reveal variability between different energies of the GCR spectrum (Fig. 2).

Cosmic rays are responsible for the ionisation in the lower atmosphere below 35 km. Atmospheric profiles of ion pair production taken during solar maximum and solar minimum can be seen in Fig. 3. The difference between max and min peaks at around 13 km and continues down to the surface.

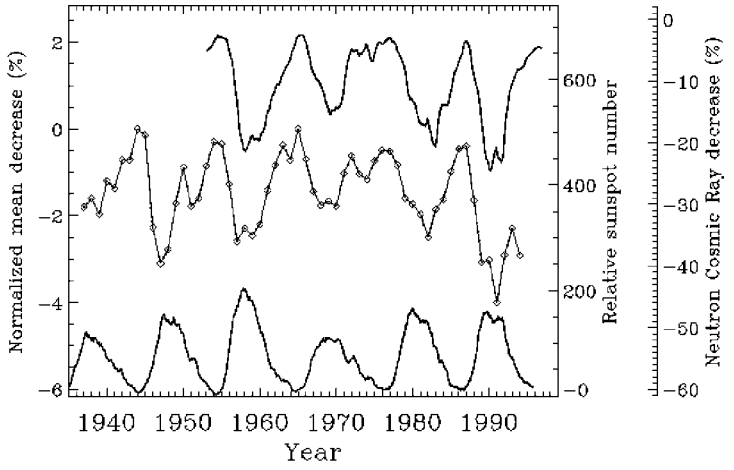

Figure 2. Temporal variability of GCR measured at the Earth surface together with the sunspot number (adapted from Svensmark, 1998). This reveals a clear solar cycle modulation of the Cosmic Ray flux. The top curve is monthly averages of GCR as measured by the CLIMAX neutron monitor (cut-off rigidity >3 GeV), Colorado (1953–1996), values have been normalised to May 1965. The middle curve is the annual mean variation in GCR captured by ionisation chambers (1934–1994), values are normalised to 1965 (adapted from Ahluwalia, 1997). The bottom curve is the relative sunspot number.

Edward P. Ney (1959) observed that atmospheric ionisation was 'the meteorological variable subject to the largest solar cycle modulation in denser layers of the atmosphere'. How this might influence climate is open to speculation, but Ney suggested a possible link might be through an influence on 'storminess'. It was not until 1997 that Svensmark and Friis-Christensen (1997) showed from observations that ionisation might be influencing global cloud cover.

2. Clouds and Cosmic Rays

Figure 4 is a composite of Satellite observations of Earth's total cloud cover from Svensmark (1998). The cloud data comprise the NIMBUS-7 CMATRIX project (Stowe et al., 1988) (triangles), and the International Satellite Cloud Climatology Project (ISCCP) (Rossow and Schiffer, 1991) (squares). Finally data from the Defence Satellite Meteorological Program (DMSP) Special Sensor Microwave/Imager (SSM/I) (diamonds) (Weng and Grody, 1994). For details see Svensmark (1998). In the figure the cloud data is compared with variation in GCR flux and the 10.7 cm radio flux from the Sun. This radio flux follows closely variations in total solar irradiance, soft X-rays, and ultraviolet radiation over this period. There are clearly differences between the variation of GCR and the radio flux with a lag of almost two years before 1987. Crucially, Earth's cloud cover follows the GCR flux more closely than the 10.7 cm flux. This observation suggests that a mechanism linking

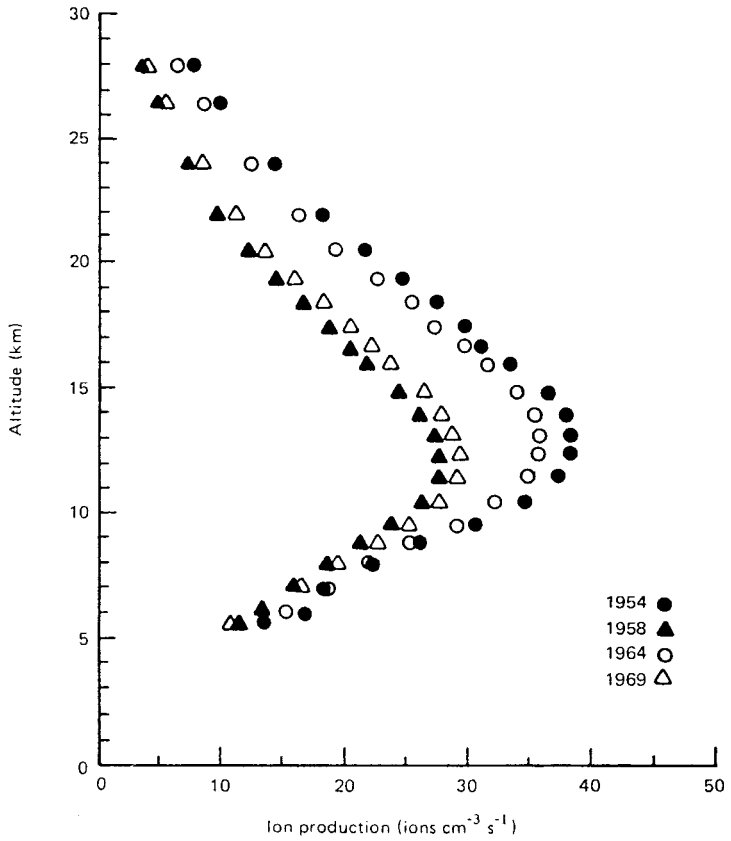

Figure 3. Variability over a solar cycle in the vertical profiles of Ion pair production over Thule, which is situated at a high magnetic latitude (adapted from Neher, 1971). Due to geomagnetic shielding, the levels of ionisation are reduced at lower latitudes, but essential features in the vertical profile are similar.

cloud cover with solar activity will involve changes in ionisation properties of the atmosphere rather than incoming solar radiation.

Clouds influence vertically integrated radiative properties of the atmosphere by cooling through reflection of incoming shortwave radiation, and heating through trapping of outgoing longwave radiation. The net radiative impact of a particular cloud is mainly dependent upon its height above the surface and its optical thickness as can be seen from Tab. I. High optically thin clouds tend to heat while low clouds, which are generally thick, tend to cool (Hartmann, 1993). With a current climatic estimate for the net forcing of the global cloud cover as a 27.7 Wm^{-2} cooling in the atmosphere, clouds clearly play an important role in the Earth's radiation budget (Hartmann, 1993; Ohring and Clapp, 1980; Ramanathan et al., 1989; Ardanuy et al., 1991). A significant solar influence on global cloud properties is potentially important for the Earth's radiation budget, but the sign and magnitude will be determined by the cloud types affected.

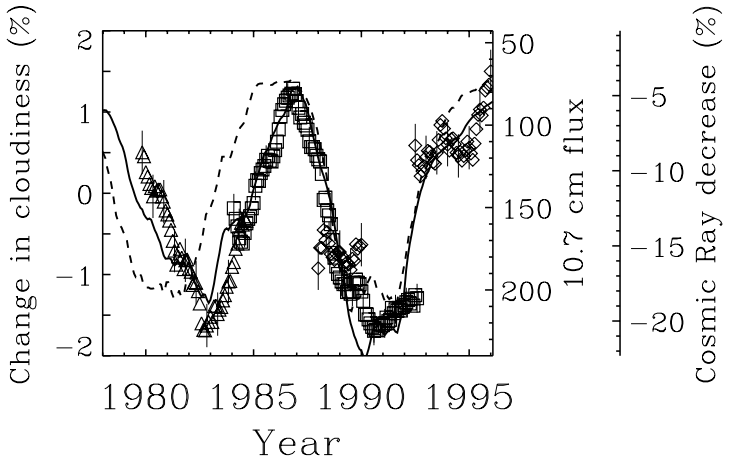

Figure 4. Composite figure showing changes in Earth's total cloud cover for four cloud data sets obtained from satellite observations. Also plotted are the cosmic rays fluxes from Climax (solid curve, normalised to May 1965), and 10.7-cm Solar flux (broken curve, in units of $10^{-22}\,\mathrm{Wm^{-2}Hz^{-1}}$). Triangles are the Nimbus-7 data, squares are the ISCCP-C2 and ISCCP-D2 data, and diamonds are the DMSP data. All the displayed data have been smoothed using a 12-month running mean. The Nimbus-7 and the DMSP data is total cloud cover for the Southern Hemisphere over oceans, and the ISCCP data have been derived from geostationary satellites over oceans with the tropics excluded.

TABLE I

Radiative forcing from ERBE experiment (adapted from Hartmann, 1993).

	High Clouds		Middle Clouds		Low Clouds	Total
	Thin	*Thick*	*Thin*	*Thick*		
Global Cloud Fraction %	10.1	8.6	10.7	7.3	26.6	63.3
Net CRF $\mathrm{Wm^{-2}}$	2.4	−7.0	1.1	−7.5	−16.7	−27.7

Recently it has been possible to observe cloud properties at different altitudes from the global dataset International Satellite Cloud Climate Project (ISCCP-D2) (Schiffer and Rossow, 1983; Schiffer and Rossow, 1985; Rossow and Schiffer, 1991; Rossow et al., 1996). These are derived from Top Of Atmosphere (TOA) radiances for the period July 1983 to September 1994. Monthly averages of infrared (IR) measurements are preferred due to their superior spatial and temporal homogeneity over visual observations that can only be detected during daylight. Cloud cover is obtained from an algorithm using the TOA IR statistics to identify the cloudiness on an equal area grid (280 km × 280 km). Cloud top temperatures (CT) and pressures (CP) are obtained from an ISCCP IR model constrained by water vapour and vertical temperature profiles retrieved from the TIROS Observed Vertical Sounder (TOVS) (Rossow et al., 1996). CT and CP are found by assuming an opaque cloud, i.e. emissivity $\epsilon = 1$, and adjusting the clouds pressure level

(effectively cloud height) in the model until the reconstructed outgoing IR flux at TOA matches that observed. Based on retrieved CP, clouds are divided into Low >680 hPa (<3.2 km), Middle $\sim$680–440 hPa (3.2–6.5 km), and High <440 hPa (>6.5 km), Fig. 5.

Clearly, GCR flux over this period is correlated with a $\sim$2% absolute change ($\sim$7% relative change) in low cloud cover, while there is no correlation with middle and high clouds. However, at these time scales GCR ionisation is not the only mechanism affecting low clouds, there are of course many other decadal processes in the climate system which are important, and one should not expect a perfect correlation. The small differences between Low cloud cover and GCR seen in Fig. 5c are much smaller than the lag between the 10.7-cm flux and total cloud cover (Fig. 4), and are close to the satellite's resolution. What is surprising is that despite these limitations a signal of solar variability in low clouds is dominant at time scales longer than 1 year. Since low clouds tend to be optically thick they are efficient reflectors of sunlight and have a negative impact on the Earth's radiation budget (Tab. I). Based on observations made under the Earth Radiation Budget Experiment (ERBE) the average low cloud radiative forcing contributes a cooling of -16.7 W/m^2. Thus a $\sim$2% absolute change in low cloud cover over a solar cycle, would give a change in net low cloud forcing of $\sim$1.2 W/m^2.

In addition to cloud cover, the IR model also generates an additional cloud parameter, cloud top temperature (CT), at Low, Mid, and High altitudes. The spatial correlation map in Figure 6 shows how low cloud top temperatures covary with GCR flux, particularly over oceans in regions where stratocumulus and marine-stratus clouds are dominant (for details see (Marsh and Svensmark, 2000). The lack of correlation at high latitudes is currently not understood, but may be related to differences in processes of cloud formation.

However, the opaque cloud assumption excludes microphysical properties and so constrains cloud variability to appear only in cloud 'model height', thus introducing an element of artificial variability into CT. Observed properties of low level maritime clouds suggests that they are not opaque (Heymsfield, 1993). Relaxing the opaque assumption allows cloud variability to manifest itself through changes in cloud optical depth, i.e., $\epsilon < 1$.

3. Clouds and Aerosols

Cloud optical depth depends on processes affecting the cloud drop size distribution, and cloud thickness which is influenced by atmospheric vertical temperature profiles. Since low clouds are warm (>273 K) they consist of liquid water drops which form on cloud condensation nuclei (CCN), and so the drop size distribution depends on the density of atmospheric aerosols activated as CCN. The abundance of CCN is determined by both the level of supersaturation and the number of aerosols present in the atmosphere able to grow into CCN. Increases in supersaturation,

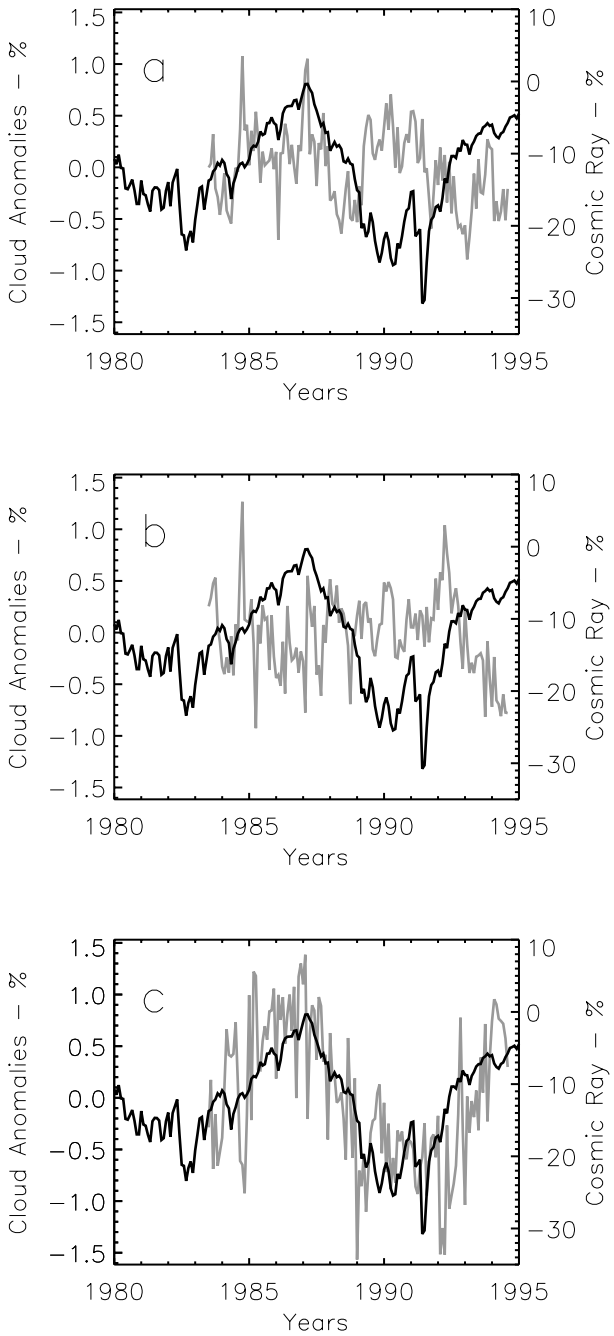

Figure 5. Monthly mean values for global anomalies of; a) high (<440 hPa), b) middle (440–680 hPa), and c) low (>680 hPa) cloud cover (gray). Galactic cosmic ray fluxes (GCR) from Climax (black, normalised to May 1965) are used as a proxy for solar variability. The global average of the temporal mean over this period for high, middle and low IR detected clouds is 13.5%, 19.9%, and 28.0% respectively.

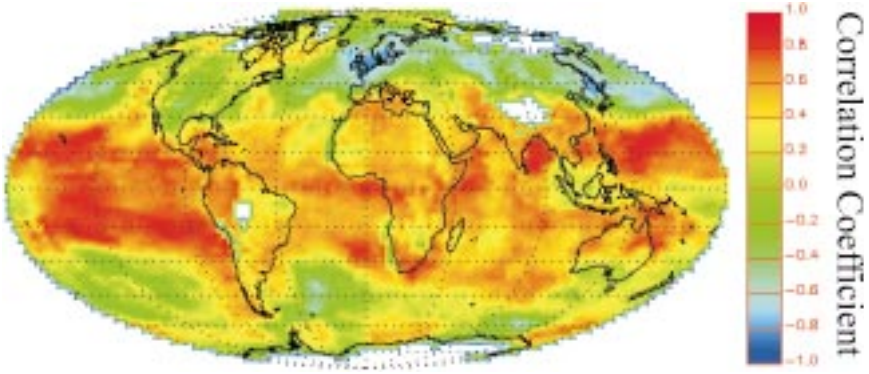

Figure 6. Global correlation map of GCR with anomalies of Low cloud top temperature (CT). The fraction of Earth possessing a correlation coefficient >0.6 is 29.6% which is significant at >99.9%.

typically between 0.1% and a few percent, activates increasingly smaller aerosols. A solar signal could enter low cloud properties through influencing atmospheric vertical temperature profiles, water vapour, or aerosol to CCN activation processes.

TOVS observations of the vertical profiles of water vapour and temperature demonstrate little correlation with GCR (Fig. 7). This suggests that solar induced variability of local thermodynamic properties in the atmosphere cannot be entirely responsible for the observed changes in low cloud properties. Since the vertical atmospheric structure depends on radiatively driven large-scale circulation, this might not be surprising given that variability in solar irradiance agrees poorly with cloud properties (Fig. 4).

4. Aerosols and Cosmic Rays

Assuming typical atmospheric water vapour saturations of up to a few percent, the abundance of CCN is determined through properties of the background aerosol size distribution ($\sim$0.1–1.0 mm). Production of aerosol can be due to many processes involving: gas-particle conversion, droplet-particle conversion, i.e., evaporation of water droplets containing dissolved matter, and bulk particles from the surface, e.g., smoke, dust, or pollen (Pruppacher and Klett, 1997). Observations of spectra in regions of low cloud formation indicate that aerosols are produced locally. In the troposphere it is believed that ionisation contributes to the gas-particle formation of ultrafine (<20 nm) aerosol, and the subsequent growth into the matured aerosol distributions which act as CCN (Turco et al., 1998; Hõrrak et al., 1998; Yu and Turco, 2000). Figure 8 shows the ionisation density profile of the atmosphere and the major ion species produced. The complexity of ions increases with decreasing altitude. It is the ions, produced within the troposphere by cosmic rays, which are potentially important for aerosol production.

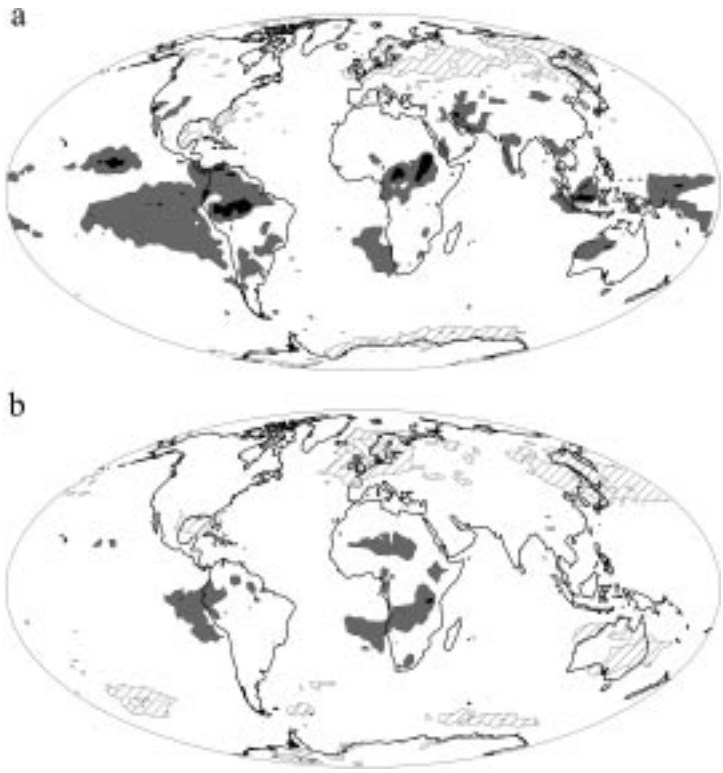

Figure 7. Global correlation maps of GCR with anomalies of a) atmospheric water vapour (1000–680 hPa), and b) atmospheric temperature at 740 hPa. The water vapour and temperature are given by TOVS observations covering the period July 1983 – September 1994 (Rossow, 1996). Anomalies and correlation coefficients are calculated as in Figs. 5 and 6 (see both figure captions). The shading corresponds to filled contours, where correlation coefficient $r > 0.8$ - black, $r > 0.6$ - grey, and $r < -0.6$ - hatched, there are no regions with $r < -0.8$. The fraction of Earth possessing a correlation coefficient > 0.6 is a) 11.7% and b) 3.4% which is not significant.

Currently it is uncertain whether variability in atmospheric ionisation due to the GCR flux could have a significant effect on either aerosol production or droplet growth. However, models have revealed that nucleation through ion-ion recombination (Turco et al., 1998) is capable of maintaining a background aerosol distribution with realistic concentrations in the troposphere, Tab. II.

This is just one possible mechanism, but it emphasises the potential importance of ionisation for troposphere aerosol production. It is not unrealistic to imagine that a systematic change in cosmic ray ionisation could lead to a change in aerosol populations acting as CCN and thus influence cloud properties.

Note that the process of aerosols acting as a source of CCN for low clouds is quite different to the source of nuclei for higher altitude ice clouds. Therefore, the influence of ionisation on aerosol processes affecting low cloud CCN need not

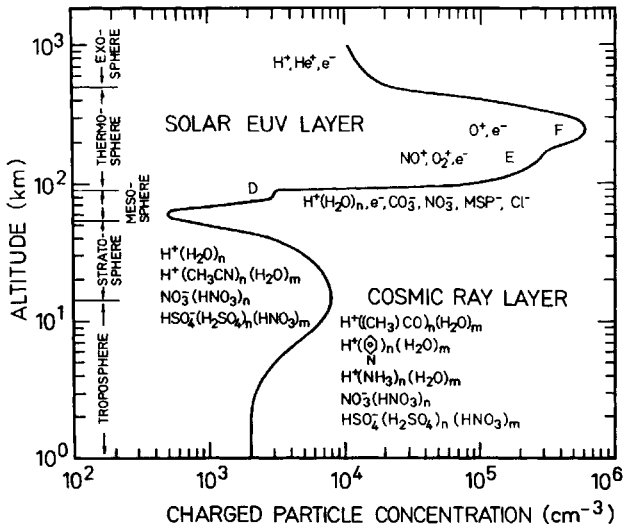

Figure 8. Vertical Profile of ionisation density in the atmosphere. Included are the major ion species at various altitudes (adapted from Viggiano and Arnold, 1995).

TABLE II
Aerosols

	Concentration - cm^{-3}
CCN in a maritime air mass at 1% supersaturation over the Pacific (Pruppacher and Klett, 1997).	∼100
Background aerosol in a maritime air over the Pacific (Pruppacher and Klett, 1997).	∼200
Background aerosol distribution maintained by ion-ion recombination (Turco et al., 1998).	∼200–500

be important for high clouds. A detailed discussion of ice nuclei can be found in Pruppacher and Klett (1997).

5. Influence of the Aerosol Distribution on Cloud Radiative Properties

The effect of increased aerosol on cloud radiative properties can be observed directly from ship tracks. Ship exhaust emits aerosol into low cloud layers thus increasing the local background aerosol. Consequently, the cloud droplet distribution is modified which influences the radiative properties of the cloud. Two satellite images at different wavelengths can be seen in Fig. 9, where a number of ship tracks are observable. In the visible (upper image), these show up as regular

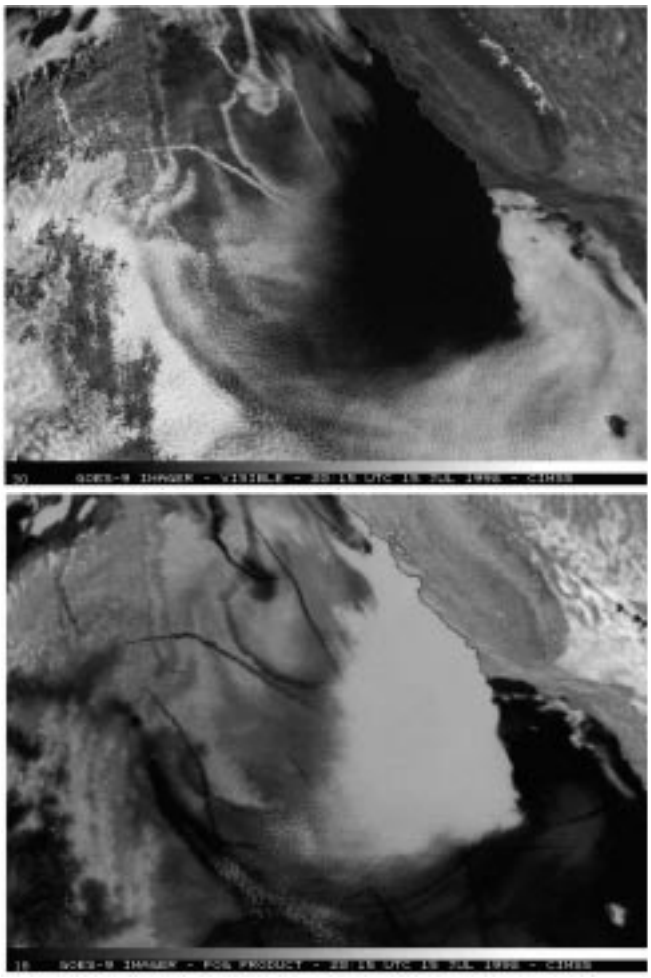

Figure 9. Images of Ship Condensation Trails Off the California Coast taken on 15 July 1998 by GOES-9. The upper image is in the visible (0.7 μm) and the lower image is the IR Fog Product (10.7 μm – 3.9 μm).

bright white lines indicating an increase in cloud albedo. The lower image is the difference between NIR and IR where the same tracks show up as dark regions. The NIR (3.2 μm) is dominated by absorption properties of the cloud while the IR (10.7 μm) is the result of the cloud emissivity. Subtracting the NIR image from the IR enhances regions of increased absorption and emission such as the dark tracks due to ship exhaust.

In-situ aircraft measurements made through shiptrack contaminated cloud give detail to the radiative changes (King et al., 1993). Figure 10 shows radiation intensities from an aircraft path through the middle of such cloud looking both in the nadir (down) and zenith (up). In the visible, the greatest influence is from backscatter

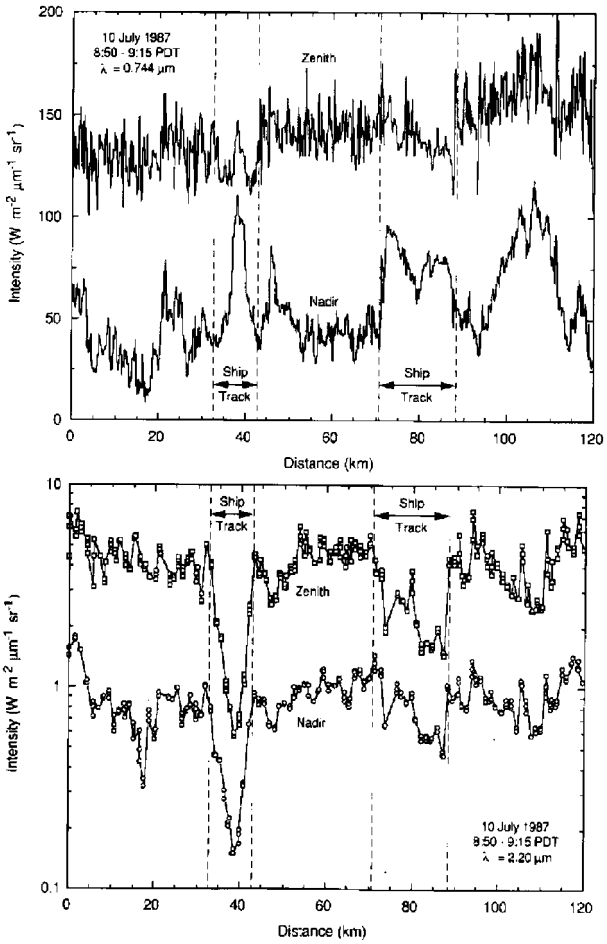

Figure 10. Visible 0.7 μm (top) and Near IR 2.2 μm (bottom) aircraft observations of ship tracks in low cloud (adapted from King et al., 1993).

below the aircraft, while the NIR reveals strong absorption both from above and below. In fact, the absorption is much stronger from above indicating the cloud is absorbing a greater flux of incoming radiation. This suggests that an increase in aerosol gives a decrease in droplet size and an increase in cloud liquid water, thus enhancing absorption of incoming radiation from above the cloud. Consequently, the cloud will heat in these regions, which explains the darkened tracks in the bottom satellite image of Fig. 9.

From the ship tracks, it is apparent that increases in aerosol leads to both an increase in albedo and an increase in absorption and therefore cloud temperature. If an increase in GCR can lead to a similar increase in aerosol, then this would explain the positive correlations between GCR and low cloud top temperatures (Fig. 7) over a large fraction of the globe.

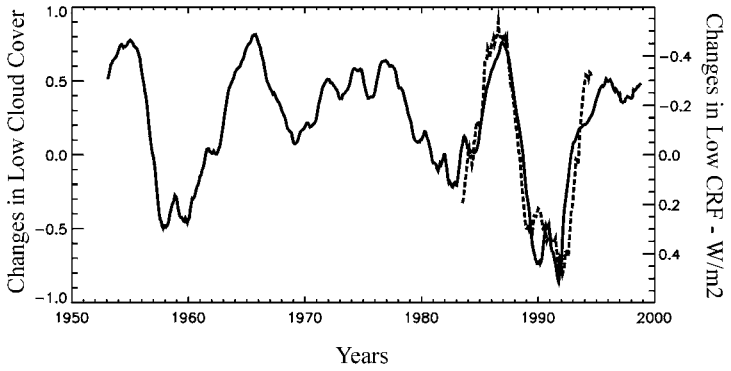

Figure 11. Reconstructed low cloud cover (solid) from galactic cosmic ray fluxes measured with a neutron counter at Huancayo (cut-off rigidity 12.91 GeV). Also shown is the 12-month smoothed global low cloud cover (dashed) from Fig. 5c. The right axis is an estimated of changes in Cloud Radiative Forcing (CRF) based on the ERBE results displayed in Tab. I. See Tab. III for estimates of long term trends in CRF from this reconstruction.

6. Estimates of Past Cloud Radiative Forcing

The radiative impact from cosmic ray influence on clouds can be extended back in time from a reconstruction assuming a linear response function (Svensmark, 1998). It was argued above, that cosmic ray ionisation in the lower troposphere affecting aerosol distributions could explain the solar variability observed in low clouds. The high-energy secondary particles penetrate the atmosphere to depths of low cloud formation, thus the Huancayo neutron counter with cut-off rigidity at 12.91 GeV is used in the reconstruction. From the following relationship:

$$\text{Reconstructed low cloud cover} = \alpha \times \text{GCR} + \beta \tag{1}$$

a history of low cloud cover is found, where α and β are obtained from a least squares fit over the period of available ISCCP low cloud data (1983–1994). The reconstructed low cloud cover is shown in Fig. 11.

Levels of cosmic rays received at Earth are influenced by the strength of the solar magnetic field. Thus, relative changes in the solar magnetic field can be used to estimate relative changes in cloud forcing. Lockwood et al. (1999) have reconstructed a history of solar source magnetic flux for the past century which agrees well with the available satellite observations for the period 1964–1995. This allows an estimate for cloud radiative forcing to be made for the period before cosmic ray observations were available. The solar magnetic field is observed to have more than doubled over the past century while at the same time cosmic radiation measured at Huancayo has decreased by 3.5% (Tab. III). Using the reconstruction of low cloud cover in Fig. 11 and the ERBE estimates for cloud radiative forcing (Tab. I) one can infer a $\sim$1.4 Wm^{-2} warming attributed to low cloud cover changes over the past century (1901–1995). This is potentially important when considering that over the same period the estimated heating from increased CO_2 emissions is $\sim$1.5 Wm^{-2}

TABLE III

Estimates of radiative heating from the reconstruction of low clouds shown in Fig. 11.

Estimated Relative Change (%) in:	Solar Max-Min 1983–1987	30-year trend 1964–1995	Century trend 1901–1995
Cosmic Ray (>12.91 GeV)	3.5	−3.5	−11.2
Solar Source Magnetic Flux		41	131
Global Low Cloud Fraction (ISCCP)	6.1	−3.5	−8.6
Net Change (Wm^{-2}) in ERBE Low CRF ($-16.7\,Wm^{-2}$)	−1.0	0.5	1.4

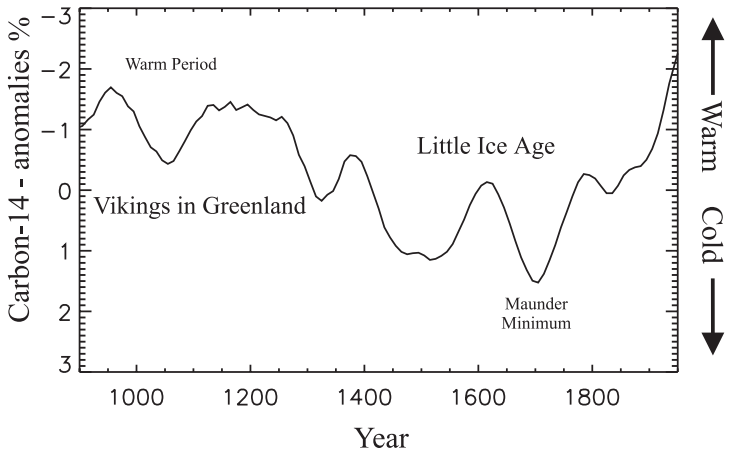

Figure 12. Changes in ^{14}C production over the past 1000 years relative to 1950. ^{14}C is produced through nuclear interactions of cosmic ray particles in the atmosphere. Cosmic rays are modulated by the solar wind; thus, variability in ^{14}C production is mainly a result of changes in solar activity. High solar activity leads to stronger shielding from the solar wind and thus a reduction in the production rate. Note the inverted axis for ^{14}C anomalies. The sharp deviation of ^{14}C during the last century is due to the burning of ^{14}C depleted fossil fuels (the Suess effect).

and changes in solar irradiance received at Earth are $0.4\,Wm^{-2}$ (Lockwood and Stamper, 1999).

A comparison between cosmic rays and climate can be extended yet further back in time, as a history of Solar activity is well known for the past 10,000 years. This is from observing changes in the production of radioisotopes in the atmosphere by galactic cosmic rays. Variations in ^{14}C production for the last millennium together with major climate epochs can be seen in Fig. 12.

Although we do not have a good estimate of the absolute global temperature record covering this period, some of the major changes in ^{14}C appear to coincide with significant climate shifts. Solar activity was particularly high from AD 1000–

1300, known as the medieval warm period, when wine was made from grapes grown in England, and the Vikings colonised Greenland. This was followed by a cold period known as the Little Ice Age, which lasted until the middle of the 19th century. During this period, the Vikings left Greenland and the River Thames regularly froze in London. The Maunder Minimum (1645–1715) was a particularly cold spell when there was a complete absence of sunspots indicating very low solar activity. This evidence suggests that in the past people experienced climate changes that have occurred in concurrence with extremes in solar variability.

7. Conclusions

Based on the ISCCP-D2 IR cloud data there is a clear correlation between solar activity and properties of low clouds in contrast to middle and high clouds. The correlation is seen in two independent parameters; a) Low cloud cover, and b) Low cloud top temperature. Observations of atmospheric parameters from TOVS do not support a solar-cloud link through tropospheric dynamics influenced by UV absorption in the stratosphere. However, since low clouds are warm and comprise of water droplets nucleated by aerosol, a link may be found through a GCR influence on the atmospheric aerosol distribution. Ship tracks suggest that low cloud radiative properties are sensitive to the background aerosol distribution such that radiative forcing due to increased aerosol leads to a warming of the cloud. If an increase in GCR can lead to similar increases in aerosol, then this would explain the positive correlation between GCR and low cloud top temperatures over a large fraction of the globe. Historical records suggest that systematic changes in global climate follow observed changes in GCR. This is consistent with low GCR corresponding to fewer low clouds and therefore a warmer climate. Crude estimates of changes in cloud radiative forcing over the past century, when the solar magnetic flux more than doubled, indicates that a GCR-cloud mechanism could have contributed $\sim 1.4\,\mathrm{Wm}^{-2}$ to the observed global warming. These observations provide compelling evidence to warrant further study of the effect of GCR on clouds.

References

Ardanuy, P., Stowe, L.L., Gruber, A., and Weiss, M.: 1991, 'Shortwave, longwave, and net cloud-radiative forcing as determined from Nimbus-7 observations', *J. Geophys. Res.* **96**, 18,537.

Geller, M.A., and Alpert, J.C.: 1980, 'Planetary wave coupling between the troposphere and the middle atmosphere as a possible sun–weather mechanism', *J. Atmos. Sci.* **37**, 1197.

Haigh, J.D.: 1996, 'The impact of solar variability on climate', *Science* **272**, 981.

Hartmann, D.L.: 1993, *Radiative effects of clouds on Earth's climate, in Aerosol-Cloud-Climate Interactions*, Academic Press.

Herman, J.R., and Goldberg, R.A.: 1978, *Sun, Weather, and Climate*, NASA SP 426.

Heymsfield, A.J.: 1993, *Microphysical Structures of Stratiform and Cirrus Clouds, in Aerosol-Cloud-Climate Interactions*, Academic Press.

Hõrrak, U., Salm, J., and Tammet, H.: 1998, 'Bursts of intermediate ions in atmospheric air', *J. Geophys. Res.* **103**, 13,909.
King, M.D., Radke, L.F., and Hobbs, P.V.: 1993, 'Optical properties of marine stratocumulus clouds modified by ships', *J. Geophys. Res.* **98**, 2729.
Lal, D., and Peters, B.: 1967, 'Cosmic ray produced radioactivity on the Earth', in *Encyclopaedia of Physics*, Springer-Verlag, Berlin.
Lean, J., Beer, J., and Bradley, R.: 1995, 'Reconstruction of solar irradiance since 1610: Implications for climate change', *Geophys. Res. Lett.* **22**, 3195.
Lockwood, M., Stamper, R., and Wild M.N.: 1999, 'A doubling of the Sun's coronal magnetic field during the past 100 years', *Nature* **399**, 437.
Lockwood, M. and Stamper, R.: 1999, 'Long-term drift of the coronal source magnetic flux and the total solar irradiance', *Geophys. Res. Lett.* **26**, 2461.
Marsh, N.D. and Svensmark, H.: 2000, 'Low cloud properties influenced by solar activity', *Phys. Rev. Lett.*, submitted.
Neher, H.V.: 1971, 'Cosmic-Rays at high latitudes and altitudes covering four solar maxima', *J. Geophys. Res.* **76**, 1637.
Ney, E.R.: 1959, 'Cosmic radiation and the weather', *Nature* **183**, 451.
Ohring, G., and Clapp, P.F.: 1980, 'The effect of changes in cloud amount on the net radiation at the top of the atmosphere', *J. Atmos. Sci.* **37**, 447.
Pruppacher, H.R., and Klett, J.D.: 1997, *Microphysics of Clouds and Precipitation*, Kluwer, Dordrecht.
Ramanathan, V., et al.: 1989, 'Results from the Earth's radiation budget experiment', *Science* **243**, 57.
Rossow, W.B., and Schiffer, R.A.: 1991, 'ISCCP Cloud Data Products', *Bull. Am. Met. Soc.* **72**, 2.
Rossow, W.B., Walker, A.W., Beuschel, D.E., and Roiter, M.D.: 1996, *International Satellite Cloud Climatology Project (ISCCP): Documentation of New Cloud Datasets*, World Meteorological Organization, Geneva.
Schiffer, R.A., and Rossow, W.B.: 1983 'The International Satellite Cloud Climatology Project (ISCCP): The first project of the World Climate Research Programme', *Bull. Am. Met. Soc.* **64**, 779.
Schiffer, R.A., and Rossow, W.B.: 1985, 'ISCCP Global Radiance Data Set: A New Resource for Climate Research', *Bull. Am. Met. Soc.* **66**, 1498.
Shindell, D., Rind, D., Balabhandran, N., Lean, J., and Lonergan, P.: 1999, 'Solar cycle variability, ozone, and climate', *Science* **284**, 305.
Stowe, L.L., Wellemayer, C.G., Eck, T.F., Yeh, H.Y.M., and the Nimbus-7 team: 1988, *J. Clim.* **1**, 445.
Svensmark, H., and Friis-Christensen, E.: 1997, 'Variation of Cosmic Ray Flux and Global Cloud Coverage – A Missing Link in Solar-Climate Relationships', *J. Atm. Sol. Terr. Phys.* **59**, 1225.
Svensmark, H.: 1998, 'Influence of cosmic rays on climate', *Phys. Rev. Lett.* **81**, 5027.
Turco, R.P., Zhao, J.-X., and Yu, F.: 1998, 'A new source of tropospheric aerosols: Ion-ion recombination', Geophys. Res. Lett. **25**, 635.
Viggiano, A.A., and Arnold, F.: 1995, *Ion Chemistry and Composition of the Atmosphere, in Handbook of Atmospheric Electrodynamics*, CRC Press.
Weng, F., and Grody, N.C.: 1994, *J. Geophys. Res.* **99**, 25,535.
Yu, F., and Turco, R.P.: 2000, 'Ultrafine aerosol formation via ion-mediated nucleation', *Geophys. Res. Lett.* **27**, 883.

Address for Offprints:
Nigel Marsh and Henrik Svensmark, Danish Space Research Institute, Juliane Maries Vej 30, DK-2100 Copenhagen Ø, Denmark, hsv@dsri.dk